MXene Reinforced Polymer Composites

Fabrication, Characterization, and Applications

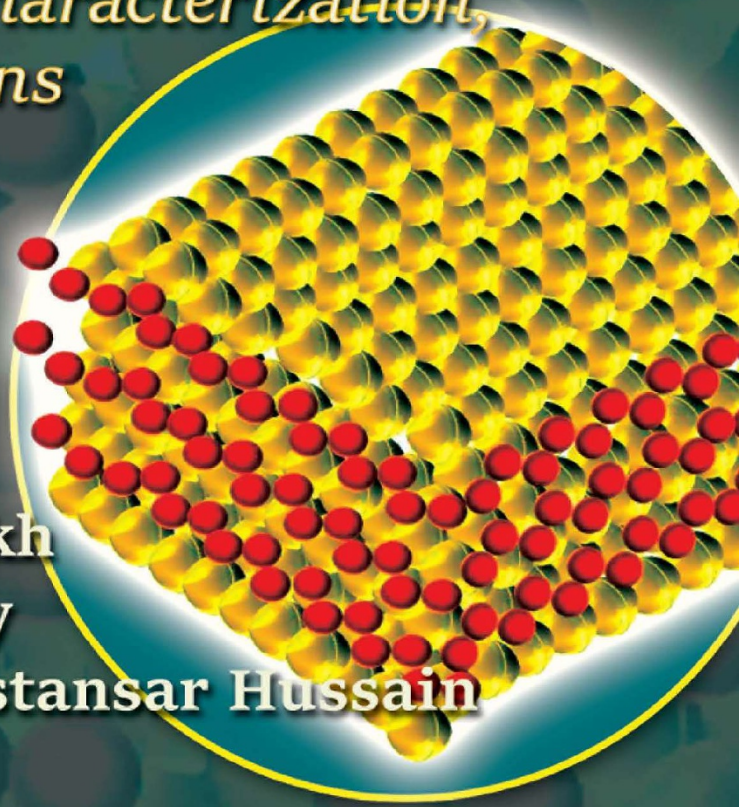

Edited by
Kalim Deshmukh
Mayank Pandey
Chaudhery Mustansar Hussain

Scrivener Publishing

WILEY

MXene Reinforced Polymer Composites

Scrivener Publishing
100 Cummings Center, Suite 541J
Beverly, MA 01915-6106

Publishers at Scrivener
Martin Scrivener (martin@scrivenerpublishing.com)
Phillip Carmical (pcarmical@scrivenerpublishing.com)

MXene Reinforced Polymer Composites

Fabrication, Characterization and Applications

Edited by
Kalim Deshmukh
New Technologies-Research Centre, University of West Bohemia, Plzeň, Czech Republic
Mayank Pandey
Department of Electronics, Kristu Jayanti College, Bengaluru, India
and
Chaudhery Mustansar Hussain
Department of Chemistry & Environmental Sciences, New Jersey Institute of Technology, Newark, New Jersey, United States

WILEY

This edition first published 2024 by John Wiley & Sons, Inc., 111 River Street, Hoboken, NJ 07030, USA and Scrivener Publishing LLC, 100 Cummings Center, Suite 541J, Beverly, MA 01915, USA

For more information about Scrivener publications please visit www.scrivenerpublishing.com.

Wiley Global Headquarters
111 River Street, Hoboken, NJ 07030, USA

For details of our global editorial offices, customer services, and more information about Wiley products visit us at www.wiley.com.

Library of Congress Cataloging-in-Publication Data

ISBN 978-1-119-90104-4

Cover images: Pixabay.Com
Cover design by Russell Richardson

Set in size of 11pt and Minion Pro by Manila Typesetting Company, Makati, Philippines

Printed in the USA

10 9 8 7 6 5 4 3 2 1

Contents

Preface

Recently, MXenes, a relatively new and exciting class of two-dimensional (2D) materials, have attracted much attention in various research disciplines. MXenes, also called transition metal carbides, nitrides and carbonitrides, exhibit various compositions and remarkable properties, such as easy dispersibility, high surface-to-volume ratio, metallic conductivity and exceptional mechanical and structural characteristics. These properties make them promising candidates to be used as nanofillers in polymer composites. Polymer/MXene composites are benefitted from the attractive physicochemical properties of MXenes and the flexibility and facile processability of polymer matrices.

This book provides a detailed discussion of fundamental characteristics, synthesis and processing methods, structure, properties and characterizations of MXenes. Furthermore, it discusses surface chemistry and functionalization strategies of MXene and their incorporation into various polymer matrices to form high-performance polymer composites, followed by a systematic review of various strategies employed to design and synthesize advanced polymer/MXene composites comprising different polymers and different types of MXenes. The book further summarizes various applications of polymer/MXene composites as dielectrics, microwave absorption and electromagnetic interference (EMI) shielding, supercapacitors and electrochemical double layer capacitors, gas and volatile organic compounds sensing, flexible wearable sensors, biomedical engineering and biomedicine, water desalination and wastewater treatment, as well as pervaporation and gas separation. This book serves as a unique resource that critically describes the important research accomplishments and findings in the area of MXene-based polymer composites, putting forth key technical challenges and future research perspectives in this field.

This book covers a comprehensive discussion on various promising aspects ranging from fundamental characteristics, synthesis, exfoliation and delamination techniques, surface chemistry, surface functionalization, and various properties of MXenes to fabrication, processing, characterizations, and numerous applications of MXene-reinforced polymer composites. The book comprises 15 chapters, which are summarized as follows.

Chapter 1 introduces 2D MXenes, their fundamental characteristics, processing, compositions, structure and various applications. Chapter 2 gives state-of-the-art recent progress in different chemical exfoliation and delamination methods of MXenes. Chapter 3 describes surface terminations, surface chemistry, and different functionalization strategies of MXenes. Chapter 4 discusses the electronic, electrical, and optical properties of MXener, while the magnetic, mechanical and thermal properties of MXenes are discussed in Chapter 5.

Chapter 6 provides information about different fabrication and processing methods and properties of MXene-reinforced polymer composites. Chapter 7 discusses the structural, morphological and tribological properties of polymer/MXene composites. Chapters 8-15 discuss various applications of MXene-reinforced polymer composites including dielectrics, microwave absorption and EMI shielding, supercapacitors and electrochemical double layer capacitors, gas and volatile organic compounds sensing, flexible wearable sensors, biomedical engineering and biomedicine, water desalination and wastewater treatment, as well as pervaporation and gas separation. Overall, this book will benefit all academic and industrial researchers who work in the emerging field of 2D MXenes and their polymer composites.

We are deeply grateful to all authors for their excellent contributions to this book. We also highly appreciate the dedicated support and valuable assistance rendered by Martin Scrivener and the Scrivener Publishing team during the publication of this book.

Dr. Kalim Deshmukh
Dr. Mayank Pandey
Prof. Chaudhery Mustansar Hussain
December 2023

1

Two-Dimensional MXenes: Fundamentals, Characteristics, Synthesis Methods, Processing, Compositions, Structure, and Applications

Sudipta Goswami and Chandan Kumar Ghosh*

School of Materials Science and Nanotechnology, Jadavpur University, Jadavpur, Kolkata, India

Abstract

During the last decade, among various two-dimensional materials, the carbides, nitrides or carbonitrides of transition metal ions (MXenes), defined by $M_{n+1}X_nT_x$ (n = 1 – 4), where M, X, and T_x stand for, respectively, the transition metal ions (e.g. Ti, V, Nb, Mo, etc.), carbon and/or nitrogen, and the surface terminated groups of different population, have drawn a lot of interest of the scientists as they exhibit unique features such as large conductivity, possibility of processing in the form of solution, large aspect ratio of the structure, and tunability of the properties. In this chapter, fundamental properties and classification of MXenes are discussed in detail along with different synthesis strategies and applications. Emphasis is given on discussing MXene hydrogel as they are widely being used in flexible electronics. Since surface functionalization plays a prominent role in this class of materials, controlling surface functionalization is discussed thoroughly. Correlation between applications of MXene and their structure is also discussed here.

***Keywords*:** MXene, MAX phase, 2D materials, surface termination, exfoliation, etching, energy storage, biomedical application

1.1 Introduction

In this chapter we discuss certain salient features of a class of two-dimensional compounds which are known by the acronym MXenes. They are composed of two-dimensional transition metal ion layers interleaved with carbon and nitrogen layers (thereby forming carbide or nitrides). The hydroxyl or oxy-halide groups are attached onto the top layers. During the last fifteen years or so, intense research is being pursued on this class of low-dimensional systems for their tremendous use in storage and harvesting of energy as well as in biomedical and sensor sectors. Among a wide range of oxide/non-oxide compounds including the lower-dimensional van der Waals solids, the MXenes (classified based on the type of transition metal ion and the number of layers) have carved a niche for themselves for their many unique features. We shall highlight those features while discussing the crystallographic and electronic structures, their synthesis and

**Corresponding author*: chandan.kghosh@jadavpuruniversity.in

Kalim Deshmukh, Mayank Pandey and Chaudhery Mustansar Hussain (eds.) MXene Reinforced Polymer Composites: Fabrication, Characterization and Applications, (1–38)

properties, and, finally, use in a score of applications. We first describe the fundamentals of these compounds along with their classification. Next, we discuss the electronic, physical, and chemical properties. The different techniques being used for synthesizing the MXenes are presented then and, different application potential of MXenes in various sectors have been discussed.

1.2 Fundamentals

The carbides or nitrides of transition metal ions in two-dimensional (2D) form are described by the general chemical formula $M_{n+1}X_nT_x$ where M, X, and T, respectively, designate the transition metal ion, carbon or nitrogen, and the hydroxyl (OH) or oxy-halide (OCl, OF, OBretc) ions which terminate the surface; 'n' defines the number of layers [1]. There are, primarily, three types of MXenes – M_2XT_x, $M_3X_2T_x$, and $M_4X_3T_x$. (Figure 1.1) [2] Interest

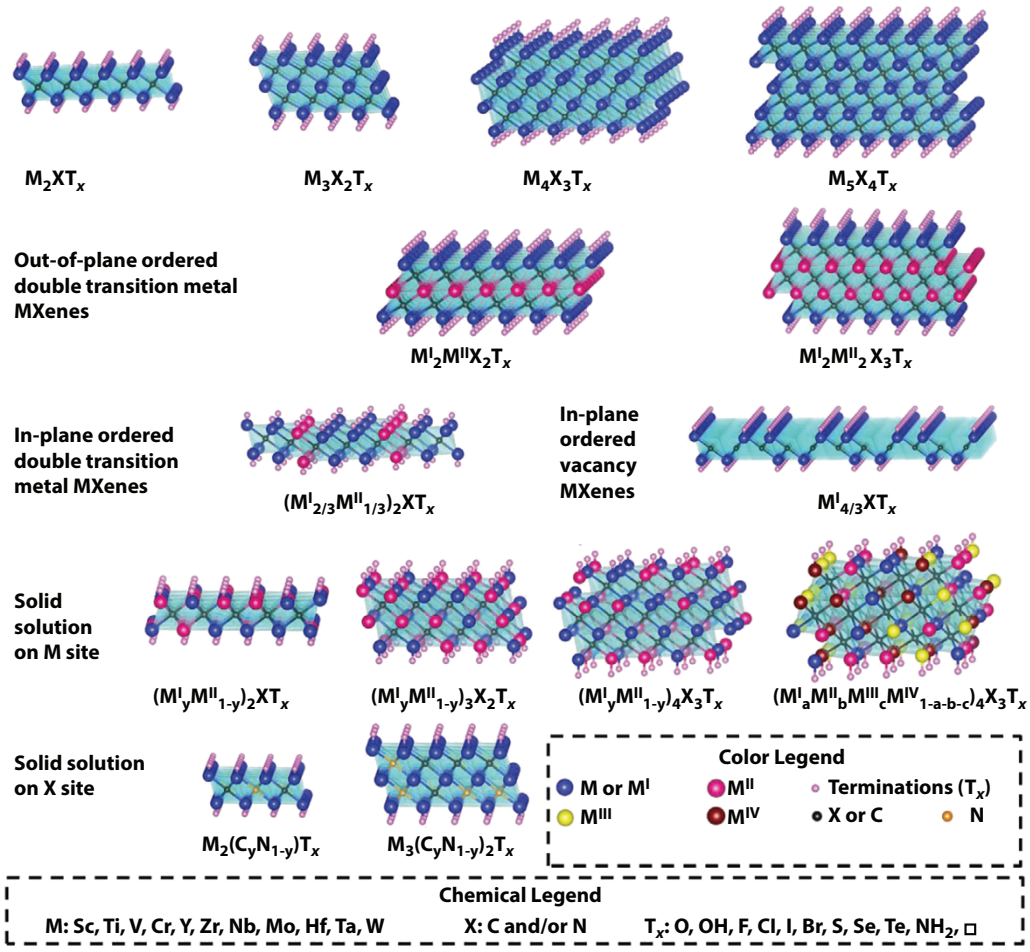

Figure 1.1 The crystallographic structure of single-, double-, and triple-layered MXene compounds $M_{n+1}X_nT_x$, (n = 1 to 4) where MX, and T represent, respectively, early transition metals, C or N, and F, O, or OH ions. More than one transition metal atoms may occupy the M sites forming solid solutions or ordered structures. Reproduced with permission from Ref. [34]. Copyright 2021, Wiley-VCH.

has been generated due to their application potential in areas such as harvesting and/or storage of energy (electrochemical supercapacitors, Li-ion, Na-ion batteries), catalysis (hydrogen or oxygen evolution reaction, CO_2 reduction), electronics/spintronics (memories, sensors), environment (membranes for clean air or water), structural, biomedical (biosensors, cancer treatment), sensors (gas, humidity, strain) etc. Unique features such as large electrical and thermal conductivity (multilayered MXenes exhibit higher conductivity than multilayered graphene), tunability of the band gap via surface terminated ions (from metallic to semiconducting), mechanical strength, etc., have made this class of compounds quite attractive for a variety of applications [3]. Here, we shall first examine their crystallographic and electronic structures for understanding the origin of the uniqueness of the properties of MXenes.

1.2.1 Crystallographic Structure

MXenes are derivatives of MAX phases where the A ions belong to the III–IV groups of the periodic table (i.e., the Al, Ga, In, Tl, Si, Ge, Sn, Pb, P, Bi, As, B, Te, S, etc.). The crystallographic structure of the MAX phase is shown in Figure 1.2 [4]. They assume hexagonal $P6_3/mmm$ (No. 194) structure [5]. By selectively leaching out the 'A' ions, it is possible to synthesize the MXenes. Therefore, the two-dimensional layers of MXenes to assume hexagonal structure (space group $P6_3/mmm$). Apart from the pure systems, alloy MXenes can also be synthesized where two different M ions – M′ and M″ – coexist and form a solid solution. In such alloy systems, ordering of the *M′* and *M″* ions have been noticed. The *M′* and *M″* ions could be ordered along the outer direction or within the planar structure [6]. In the case of ordering along the outer direction, the M′(M″) ions could be on the outermost layers while the M″(M′) ions occupy the inner layers. In the case of in-plane ordering,

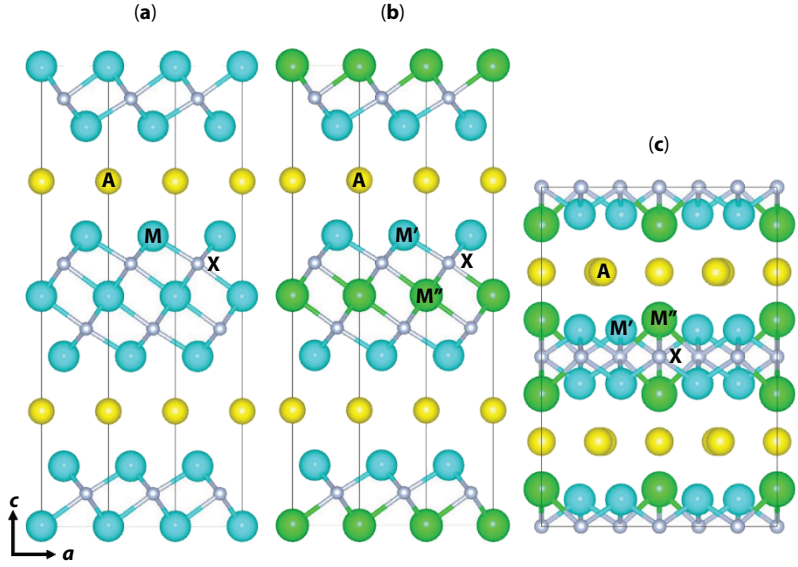

Figure 1.2 The crystal structures of the (a) MAX [M_3AX_2] phase and (b) out-of- and (c) in-plane ordered $M'_2M''AX_2$ phases. Reproduced with permission from Ref. [83]. Copyright 2019, Elsevier.

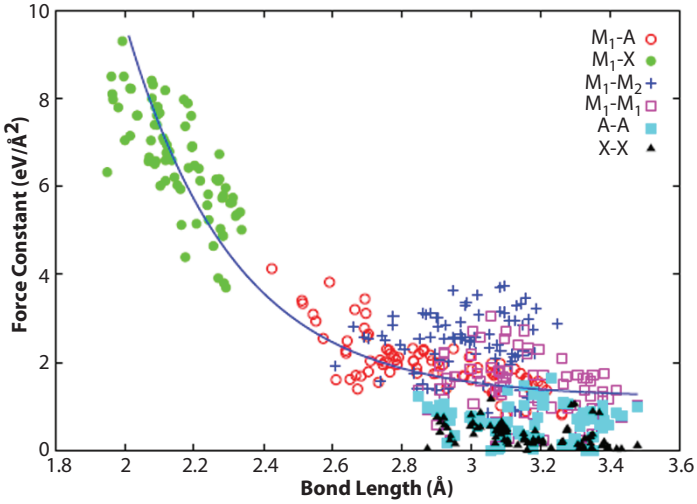

Figure 1.3 Variation of the force constant with bond length in various MAX phases. Reproduced with permission from Ref. [9]. Copyright 2018, The Royal Society of Chemistry.

the M′ and M″ ions are ordered within each layer– inner and outer. However, the in-plane ordering of M′ and M″ ions can be different from the hexagonal structure and close to the Kagome structure [7] when the size of M′ and M″ ions differ and the size of M′ ion turns out to be smaller than that of M″ ions. The space group in such cases becomes C2/c (monoclinic). The derivation of MXenes from the MAX phases requires mechanical or chemical exfoliation. The HF treatment, for example, yields formation of AF_2 and H_2 as the longer M-A bonds are relatively weak than the shortest M-X bonds. Theoretical simulation [8, 9] of the bond strengths (Figure 1.3) and the exfoliation processes offers insights behind the exfoliation processes. The MXenes also contain the F, OH, O surface ions. During the exfoliation process, vacancies are generated at the X-sites below the M layers. As a result, two sites – one with an X ion and another without (i.e., with a vacancy) – are generated. The F, OH, O groups are adsorbed at the vacancy sites and, thereby, form the stable structure with octahedral field of transition metal M ions.

1.2.2 Electronic Structure

Most of the MXenes are either metals or semimetals or semiconductors where spin-orbit coupling (SOC) does not have any significant effect on the electronic bands. In fact, when the functionalization of the surface is absent, the pristine MXenes are metallic. In these cases, the Fermi energy lies on the d-bands of the M ions. Surface functionalization by F, OH, O ions leads to the formation of new bands with hybridization of M d bands. The Fermi energy then shifts to the gap between M d bands and X p bands and the compound becomes semiconducting [10]. Such an observation has been made in the cases of Sc_2CT_2 (T = O, OH, F) and M_2CO_2 (M = Ti, Zr, Hf). In the cases of (M′, M″)XT_x systems, Fermi energy shifts to the gap generated from d band splitting due to octahedral crystal field and,

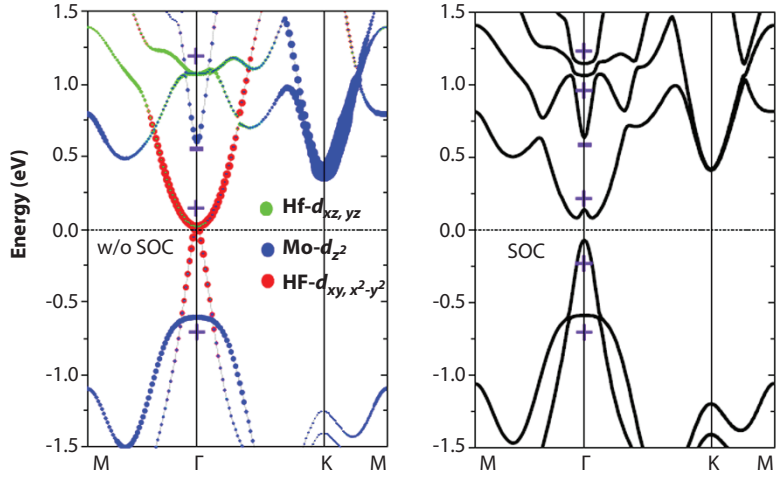

Figure 1.4 The electronic band structure of $Mo_2HfC_2O_2$ with and without spin-orbit coupling (SOC). Reproduced with permission from Ref. [11]. Copyright 2016, The American Chemical Society.

as a result, the compounds exhibit semiconducting behavior with finite energy gap. In general, single layer MXenes could exhibit semiconducting property whereas the double- or triple-layer ones are primarily metallic. However, in some cases, the SOC plays a significant role. When SOC is not present, the valence and the conduction bands (comprising of the d levels of the M ions) touch at the Γ point and give rise to semimetallic behavior. SOC splits the bands and opens a gap at the Γ point (Figure 1.4) [11]. The compounds M_2CO_2 (M = W, Mo) and $M_2'M''CO_2$ (M′ = Mo, W; M″ = Ti, Zr, Hf) exhibit such two-dimensional topological semimetallic or insulator behavior with topologically protected states with conducting edges which remain robust against nonmagnetic impurities and disorder [11].

1.2.3 Magnetic Structure

The MXenes exhibit finite magnetism and magnetic order depending on the electron states, band splitting, spin-orbit coupling, etc. For example, most of the compounds containing Cr and/or Mn exhibit magnetic order [12]. If the nonbonding d orbital resides in between bonding and anti-bonding orbitals and the Fermi level passes through these levels, finite magnetism is predicted. Theoretical calculations [13] predicted magnetism in a score MXene compounds such as M_2X (M = Ti, V, Cr, Ni, Mn; X = C, N), M_2MnC_2 (M = Ti, Hf), M_2TiX_2 (M = V, Cr, Mn), Hf_2VC_2, and $Mo_3N_2F_2$. The crystal field of the surrounding ligands of the transition metal ions determines the splitting of the bands including that of the spin bands and thus gives rise to the formation of majority and minority carriers. Accordingly, the compound exhibits metallic, half-metallic, or semiconducting properties. Most of the compounds exhibit antiferromagnetic ground state while the ones containing Mn ions are ferromagnetic. Presence of finite spin-orbit coupling in $Hf_2VC_2F_2$, on the other hand, induces noncollinear ordering with 120° rotation among the near-neighbor spins [14].

1.3 General Characteristics of the MXenes

1.3.1 Physical Properties

Some of the MXenes such as Sc_2CO_2 exhibit finite ferroelectric polarization [15] both along in- and out-of-plane directions because of asymmetric O ion cage structure. The O ions occupy the vacant sites below which C ions are present in one side and absent in another side and thus create structural noncentrosymmetry. The $(M'_{2/3}M''_{1/3})_2CO_2$ (M' = Mo, W; M'' = Sc, Y) compounds exhibit finite piezoelectric coefficient d_{11} ranging from 4 to ~25 pVm^{-1} [16] which is comparable to that of the dichalcogenides such as MoS_2, $MoSe_2$. Therefore, these compounds may find application in transducer device industry.

Some of the semiconducting compounds such as Sc_2CT_2 (T = O, OH, F) and M_2CO_2 (M = Ti, Zr, Hf) exhibit large thermoelectric power [17] because of reasonably high electrical conductivity (σ) and large Seebeck coefficient (S). The thermal conductivity (κ), on the other hand, is in the 10–60 $W.m^{-1}.K^{-1}$ range which is comparable to that of the dichalcogenides. As a result, the thermoelectric figure of merit ZT ($=S^2\sigma T/\kappa$) for these compounds approaches a high value of ~1.1.

Very interestingly, the Mo_2C is found to be superconducting with $T_c < 4$ K [18]. This compound is derived from the MAX phase Mo_2GaC which also exhibits superconductivity at T_c ~4 K [19]. Influence of the surface terminated ions such as O, F, OH, H, Br, S, Se, etc. on the superconducting transition temperature has been theoretically estimated. The compound with H and Br were predicted to exhibit a higher T_c of ~13 K [20]. These systems appear to fall in the category of Bardeen-Cooper-Schrieffer (BCS) superconductors.

The functionalization of the MXenes by different surface terminated ions (e.g., by F, O, OH etc.) gives rise to change in the optical properties because of the formation of the defect states at close to the Fermi energy. The absorption, transmittance, reflectivity characteristics change and, as a result, the compounds become suitable for various optical applications. For example, O terminated Ti_3C_2 exhibits more prominent peaks in the real part of the dielectric permittivity $\varepsilon'(\omega)$ at the frequencies below the visible light range in comparison to the F or OH terminated compounds [21]. The O-functionalized M_2C (M = Ti, Zr, Hf) also exhibits distinct absorption peaks [i.e., peaks in the imaginary part of the dielectric permittivity $\varepsilon''(\omega)$] in the visible light range. This makes them suitable for optical devices. Figure 1.5 shows the dielectric permittivity (real and imaginary) versus energy (frequency) for pristine, O, F, and OH functionalized Ti_3C [21]. The complex dielectric permittivity exhibits anisotropy [22] as well – along in- and out-of-plane directions [Figure 1.5(b)]. MXenes such as V_2CT_x (T = O, OH, F) with large absorption in the 500–2700 nm range and high conductivity are also very good candidates for applications as conductive transport electrodes.

1.3.2 Chemical Properties

The surface functionalization changes the work function (difference in Fermi energy level and the vacuum) and also the dipole moments at the surface. The changes in the work function and surface dipole moment (ΔW and ΔP, respectively) are found to maintain linear correlation. Because of such changes, the interface developed between two-dimensional MXenes and other such two-dimensional systems could give rise to Schottky-barrier-free regions [23]. By varying the surface terminated ions – O, F, OH – it is possible to reconstruct

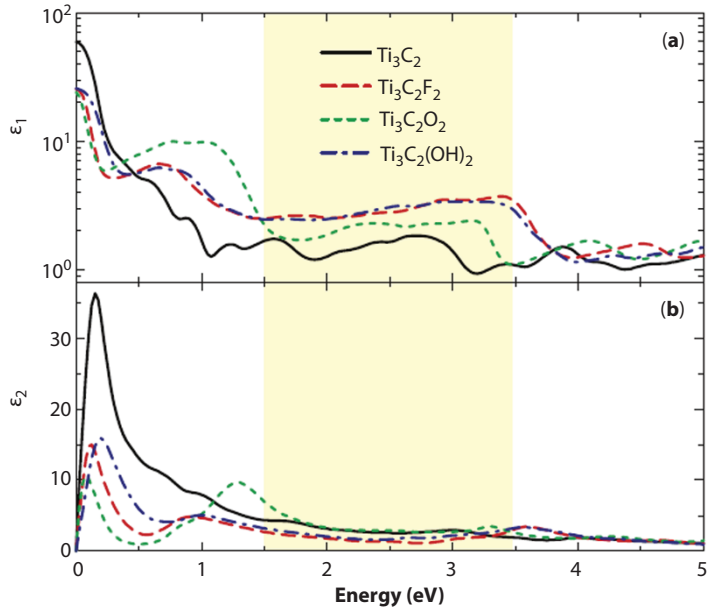

Figure 1.5 (a) The dielectric permittivity (real and imaginary) versus energy (frequency) for pristine, O, F, and OH functionalized Ti_3C_2; (b) in- and out-of-plane imaginary part of the dielectric permittivity for O-functionalized Ti, Hf, and Zr MXenes. Reproduced with permission from Ref. [21]. Copyright 2016, AIP Publishing.

the work function and thus the corresponding MXene can be made suitable for gas sensor applications [24] irrespective of their thickness (n = 1–3).

Since the surface area is large which results in enhanced surface activities, the MXenes are suitable for catalytic applications, especially, water splitting as well as hydrogen and oxygen evolution reactions (HER and OER) at the cathode and anode, respectively. The Gibbs free energy corresponding to the hydrogen absorption is close to zero for O-terminated Ti_2CO_2 and W_2CO_2. This has made them suitable for HER [25]. A theoretical calculation shows that among all the MXenes, the Mo_2CT_x possesses the most suitable surface activity for HER. Introducing metal ions (i.e., less electronegative) such as Fe it is possible to enhance the HER even further as the charge transfer to the O ions weakens the O-H bonds in water and thus facilitates the HER. The hybrid structure Ti_3C_2/g-C_3N_4 improves the OER [26], on the contrary, as the charge transfer between Ti and carbon nitride in graphitic form facilitates the oxygen evolution.

MXenes are potential candidates for energy storage (e.g., as capacitors and batteries) because of their large surface area and electrical conductivity. The diffusion barrier for selective ions can be engineered suitably by functionalizing the surface by O, F, or OH ions in various MXene compounds. For example, the diffusion barrier for Li ion can be changed [27] by introducing defect states in Ti_2C system and/or by developing hybrid structure with graphene. The Ti_2CT_2 (T = O, OH)/graphene heterostructure offers higher barrier for the diffusion of Li ions than what is observed in the pristine and monolayered MXene. The diffusion of alkali ions such as Na and K has also been studied in such structures [28]. It has been found that these monovalent ions diffuse more effectively than the multivalent Mg, Ca, Al ions. Monolayer MXene such as Ti_2C is found to be suitable for hydrogen adsorption

as well [29]. The hydrogen adsorbed form hydrides whereas in the cases of double or triple layered compounds, molecular hydrogen was found to form.

1.4 Synthesis Methods

MXenes was first prepared from its corresponding MAX phase by removing "A". It produces two-dimensional (2D) flakes of general formula $M_{n+1}X_nT_x$ (n = 1, 2, 3). After the etching of "A", the surface terminations, T_x, cover the produced sheet. M stands for ions such as Ti, Nb, Cr, Mo, etc., X represents carbon and/or nitrogen which are connected with layers of group IIIA or IVA atoms and T stands for fluorine (F), hydroxyl (OH), or oxygen (O) ions

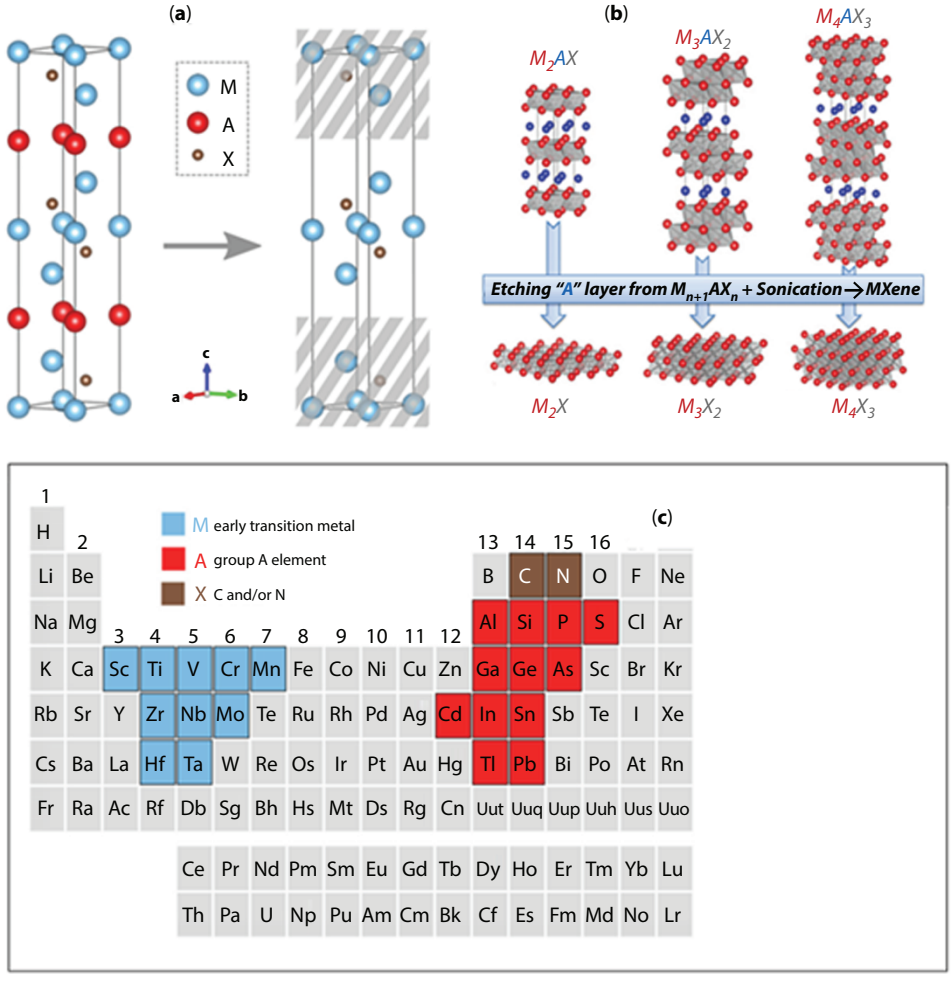

Figure 1.6 (a) The M_3AC_2 MAX phase primitive cell (left panel), and the resulting M_3C_2 MXene primitive cell (right panel). The blue spheres stand for the M atoms, the red for A atoms, and the brown for C atoms; (b) Structure of MAX phases from the corresponding MXenes after etching; (c) the location of the components of a MAX phase in the periodic table. Reproduced with permission from Ref. [30]. Copyright 2020, AIP Publishing.

which terminate the surface [30] (Figure 1.6). The selective elimination of element "A" can be achieved by two different ways – either top-down or bottom-up techniques. The top-down method basically includes liquid based etching process and is widely utilized. The bottom-up method, on the other hand, forces assembling of small atoms/molecules into 2D structures of different patterns. They include the CVD, carbonization etc. Different kinds of synthesis strategies for making 2D MXenes have been reported so far; e.g., wet selective etching, chemical vapor deposition (CVD), plasma-enhanced pulsed laser deposition (PEPLD), template method, intercalation etc. and discussed in details in following sections.

1.4.1 Wet Chemical Etching

The strategy for the preparation of 2D MXenes via wet selective etching involves the engraving of atomic layers of "A" from a multilayered MAX phase at room temperature. The higher reactivity of "A" and the weaker M-A bonds (than the layer-to-layer M-X bonds) are the key driving forces in this reaction [31]. In this process (Figure 1.7a) [32] etchant like aqueous HF of specific concentration is mixed with MAX phase powder by vigorous stirring for a specified time. HF breaks down the weak M-A bonds easily. Upon the removal of A-layer, interaction between the 2D sheets is weakened. Therefore, one can separate the layers very easily by ultrasonication or centrifugation and/or filtration [33–35]. The solid precipitate containing MXene phase is thoroughly washed with deionized water (DI) and the final pH of the suspension is maintained in between 4 to 6. The etching reaction converts the dense solid MAX phase into a loosely packed accordian-like MXenes phase; which looks alike exfoliated graphite [36]. The mechanism of etching process for Al-based MAX phase can be represented as follows:

$$M_{n+1}AlX_n + HF \rightarrow M_n{+}1X_n + AlF_3 + 1.5H_2 \tag{1.1}$$

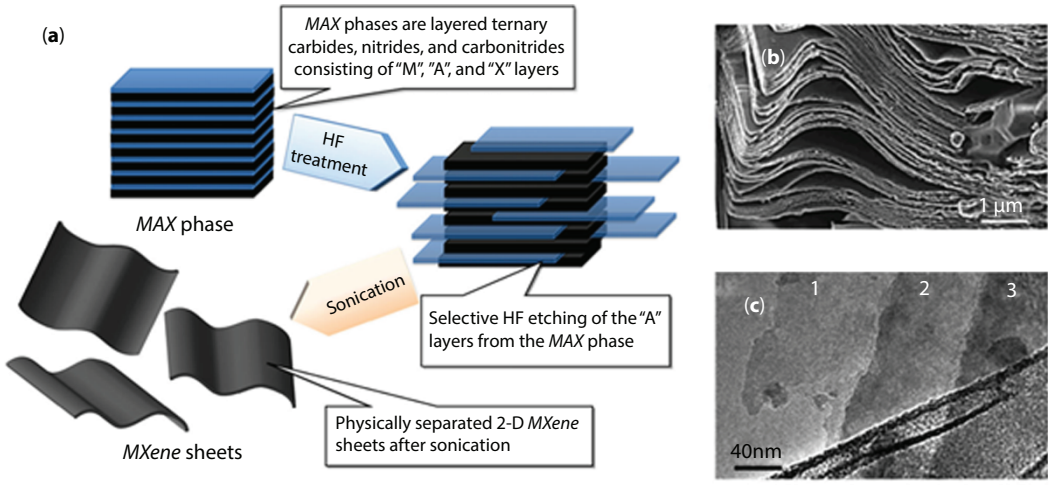

Figure 1.7 (a) Schematic for the formation of MXenes from of MAX phases by exfoliation process and; (b) The stacking of the multi-layer and (c) single layer MXenes. Reproduced with permission from Ref. [32]. Copyright 2012, The American Chemical Society.

$$M_n+1X_n+ 2H_2O \rightarrow M_n+1X_n(OH)_2+ H_2 \quad (1.2)$$

$$M_{n+1}X_n+ 2HF \rightarrow M_n+1X_nF_2+ H_2 \quad (1.3)$$

Numerous reports are available in literature for preparation of MXenes using the above principal; for example, Naguib *et al.* reported the replacement of Al atom with hydroxyl, Oxygen or Fluorine terminated surfaces from the bulk Ti_3AlC_2 by using aqueous HF. The resulting $M_{n+1}X_n$ shows a graphene like single sheet [37]. The etching process ultimately controls the defects concentration and surface termination reaction resulting in different morphology of the product; the concentration of etching solution, etching time, ultrasonic time etc. can be varied to obtain desirable microstructure like single layer or multilayer MXenes with high aspect ratio (Figures 1.7b and c). MXenes with more than 20 different compositions and stacking can be achieved by varying these process conditions. Different MXenes needs different etching time to complete the etching reaction because the etching process is dynamically controlled; with the increase in chain length (n) of MXenes a stronger and larger etching time is necessary for the complete conversion. In general, stability of the Mxene enhances with the rise in 'n'. Anasori *et al.* [38] have shown that with the increase in chain length in $Mo_2Ti_2AlC_2/Mo_2Ti_2AlC_3$ (from n = 2 to n = 3), the etching time doubles keeping all other parameter constant and Ti_2AlC requires 50% HF to yield Ti_3C_2, whereas, Ti_2AlC requires 10% HF to yield Ti_2C [32]. The combined effect of HF concentration and reaction time on the exfoliation of Al-containing MAX phases [e.g., Ti_2AlC, Ta_4AlC_3, $(Ti_{0.5}Nb_{0.5})_2AlC$, $(V_{0.5}Cr_{0.5})3AlC_2$, and Ti_3AlCN] has been studied in detail [39]. The MAX powder was immersed in different concentration of HF at room temperature. The reaction time was varied between 10 to 72 hrs. The etching reaction details are tabulated in Table 1.1. Importantly, it is noted that even after 65 h in a 50% HF solution, the reaction of the $(V_{0.5}Cr_{0.5})_3AlC_2$ powder was not complete; for all other cases the yields are quite high. The wide variation of etching parameters to remove the same element, here it is "Al" may also lie in the difference of M-Al bond energies of the corresponding MAX phase. For example, the Ti–Al bong energy (0.98 eV) in Ti_2AlC is much higher than the Nb-Al bond energy (1.21 eV) in Nb_2AlC [42]. This difference has been reflected in the longer etching time and higher HF concentration requirement for etching Al from Nb_2AlC compared to Ti_2AlC.

The SEM images of MAX phases and MXenes produced after exfoliation are shown in Figure 1.8. The figures reveal that the exfoliation of individual particles is quite successful. The importance of etching process parameters has also been reflected in an atomically laminated i-MAX phase, $(Mo_{2/3}Y_{1/3})_2AlC$, in which two different replaceable transition metal ions (Al and Y) are present in the basal plane. $(Mo_{2/3}Y_{1/3})_2AlC$ MAX phase when treated with different etching protocols gives two different types of MXene phases. Removal of Al atoms, selectively, by dissolving 1 gm $(Mo_{2/3}Y_{1/3})_2AlC_2$ into20 ml of 48%HF at room temperature with a stirring time of 12 h produces $(Mo_{2/3}Y_{1/3})_2C$ phase with in-plane elemental ordering. In another approach, removal of both Al and Y atoms have been achieved by dissolving 1 g of $(Mo_{2/3}Y_{1/3})_2AlC_2$ in 20 ml of 10 wt% HF at room temperature with a stirring time of 72 h, producing $Mo_{1.33}C$ with ordered vacancies [43]. Using liquid exfoliation via intercalation of molecules it is possible to prepare Mxenes. Introduction of appropriate molecules expands the interlayer space and weakens the interaction between layers. It eventually splits the multilayers into single sheets (Figure 1.9) [44].

Table 1.1 Reaction conditions and unit cell c-axis parameter of the of MXenes synthesized from corresponding MAX phases.

			RT etching conditions		C lattice parameter (Å)		Domain size (nm)	Yield (wt %)	Ref.
MAX structure	MAX	MXene	HF conc. (%)	Time, h	MAX	MXene			
211	Ti_2AlC	Ti_2CT_X	10	10	13.6	15.04	6	60	[32]
	V_2AlC	V_2CT_X	50	8	13.13	23.96			[40]
				90		19.73			
	Nb_2AlC	Nb_2CT_X	50	90	13.88	22.34			[40]
	$(Ti_{0.5}Nb_{0.5})_2AlC$	$(Ti_{0.5}Nb_{0.5})_2CT_x$	50	28	13.79	14.88	5	80	[32]
312	Ti_3AlC_2	$Ti_3C_2T_X$	50	2	18.42	20.51	11	100	[33, 32]
			40	20	18.62	20.89			[41]
	$(V_{0.5}Cr_{0.5})_3AlC_2$	$(V_{0.5}Cr_{0.5})_3C_2T_X$	50	69	17.73	24.26	28	NA	[32]
	Ti_3AlCN	Ti_3CNT_X	30	18	18.41	22.28	7	80	[32]
413	Ta_4AlC_3	$Ta_4C_3T_X$	50	72	24.08	30.34	38	90	[32]
	Nb_4AlC_3	$Nb_4C_3\ T_X$	50	90	24.19	30.47			[40]

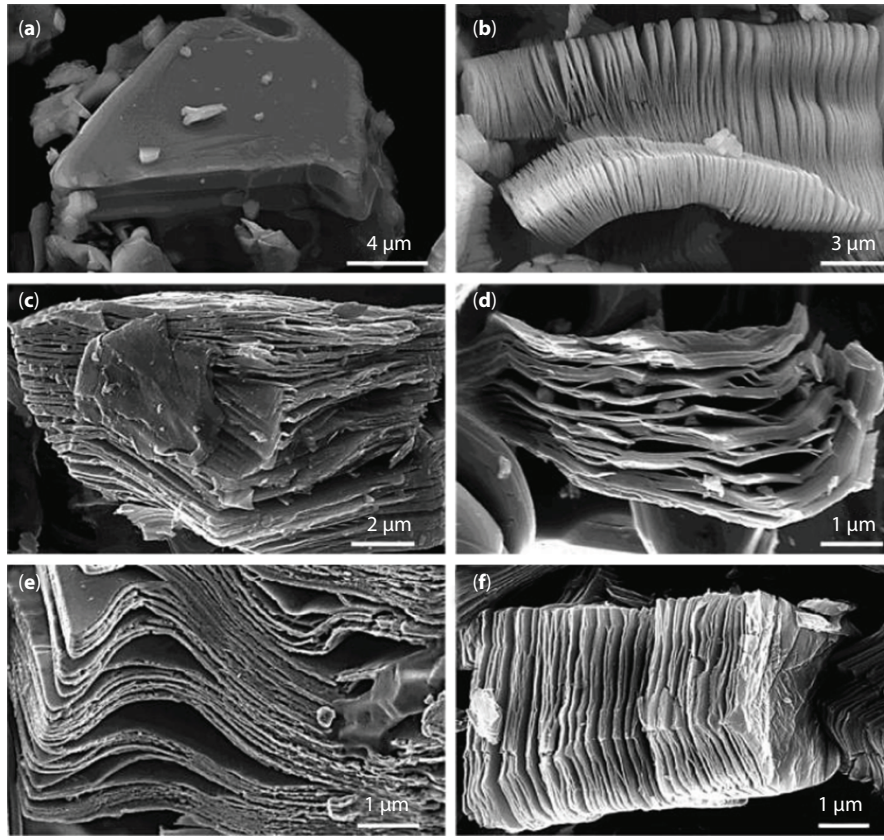

Figure 1.8 SEM images of (a) a typical unreacted Ti_3AlC_2 MAX phases before HF treatment, the exfoliation is obvious in the reaction thus producing (b) Ti_3AlC_2 (c) Ti_2AlC (d) Ta_4AlC_3 (e) TiNbAlC and (f) Ti_3AlCN "MXenes". Reproduced with permission from Ref. [32]. Copyright 2012, The American Chemical Society.

The exfoliation and intercalation can be done by using proper ultrasonication technique [45]. The etching time of Ti_3AlC_2 powders by using 49% HF could be reduced from 24 h to 4 h by using ultrasonic irradiation [46]. Ultrasonic vibration of high intensity breaks the MXene flakes into smaller sheets and facilitates the etching process. Zhang *et al.* [47] reported ultrasonication driven exfoliation of $Ti_3Si_{0.75}Al_{0.25}C_2$ using different solvents. They observed that the exfoliation is possible only if the A layer is composed of different atoms. This technique, however, cannot exfoliate pure Ti_3SiC_2. Thickness of the exfoliated ultrathin sheets is found to be ≈ 4 nm while the lateral dimensions are 100–200 nm. Obviously, intercalation increases the lattice parameter c (Δc), and the increment depends on the size of molecule of the solvent used; for $Ti_3C_2T_x$, it rises from 0.7 Å (for sodium sulphate) to 15.4 Å [for dimethyl-sulfoxide (DMSO)] [44, 48]. If ambient moisture co-intercalates spontaneously in DMSO intercalated $Ti_3C_2T_x$, it increases the c-axis parameter to a large extent and it can be further increased by storing the DMSO intercalated sample in ambient condition for long time. In general, the strategy for the preparation of $Ti_3C_2T_x$ at room temperature with HF or in-situ HF to produce delamination of multi-layered MXenes using different kinds of intercalants are tabulated in Figure 1.10 [37].